1 **Accumulation, speciation and localization of silver nanoparticles in the earthworm *Eisenia fetida***

2

3 **Pauline Courtois[1]**, Agnieszka Rorat[1], Sébastien Lemiere[1], Clément Levard[2], Perrine Chaurand[2], Anna

4 Grobelak[3], Christine Lors[1] and Franck Vandenbulcke[1*]

5

6 *[1] Univ. Lille, IMT Lille Douai, Univ. Artois, Yncrea Hauts-de-France, ULR 4515, - LGCgE, Laboratoire de*

7 *Génie Civil et géo-Environnement, F-59000 Lille, France*

8 *[2] Aix Marseille Univ, CNRS, IRD, INRAE, Coll France, CEREGE, Aix-en-Provence, France*

9 *[3] Institute of Environmental Engineering, Faculty of Infrastructure and Environment, Czestochowa University of*

10 *Technology, Czestochowa, Poland*

11

12 *Address correspondence to: Franck Vandenbulcke

13 e-mail: franck.vandenbulcke@univ-lille.fr

14 Université de Lille, Sciences et Technologies

15 Laboratoire de Génie Civil et géo-Environnement, LGCgE EA4515

16 Cité Scientifique, Bât. SN3 – F-59655 Villeneuve d´Ascq

17

18

19

28

29

30

31   ABSTRACT

32

33   The use of silver nanoparticles (AgNPs) in agriculture and many consumer products has led to

34   significant release of Ag in the environment. Although Ag toxicity in terrestrial organisms has been studied

35   extensively, very little is known about the accumulation capacity and coping mechanisms of organisms in Ag-

36   contaminated soil. In this context, we exposed *Eisenia fetida* earthworms to artificial OECD soil spiked with a

37   range of concentrations of Ag (AgNPs or $AgNO_3$). The main aims were to (1) identify the location and form of

38   accumulation of Ag in the exposed earthworms and (2) better understand the physiological mechanisms involved

39   in Ag detoxification. The results showed that similar doses of AgNPs or $AgNO_3$ did not have the same effect on

40   *E. fetida* survival. The two forms of Ag added to soil exhibited substantial differences in speciation at the end of

41   exposure, but the Ag speciation and content of Ag in earthworms were similar, suggesting that biotransformation

42   of Ag occurred. Finally, 3D images of intact earthworms obtained by X-ray micro-computed tomography

43   revealed that Ag accumulated preferentially in the chloragogen tissue, coelomocytes and nephridial epithelium.

44   Thus, *E. fetida* bioaccumulates Ag, but a regulation mechanism limit its impact in a very efficient manner. The

45   location of Ag in the organism, the competition between Ag and Cu, and the speciation of internal Ag suggest a

46   link between Ag and the thiol-rich proteins that are widely present in these tissues, most probably

47   metallothioneins, which are key proteins in the sequestration and detoxification of metals.

48

49   Keywords

50   Silver, nanomaterials, earthworm, accumulation, speciation, X-ray absorption spectroscopy, X-ray micro-

51   computed tomography

52

1. INTRODUCTION

Due to advances in nanotechnology and the increasing use of nanomaterials, metallic silver nanoparticles (AgNPs) are an emerging contaminant in the terrestrial environment (McGillicuddy et al., 2017). The incorporation of AgNPs in consumer products is increasing due to their unique properties, particularly their antimicrobial effects (Vance et al., 2015). Most silver (Ag) release occurs in municipal wastewater, and wastewater treatment plants allow efficient sequestration of Ag in sewage sludge (Kaegi et al., 2011). However, the Ag species trapped in these biosolids are subsequently spread on agricultural soil when sludge is recycled as fertilizer (Usman et al., 2012). A number of studies have shown that metallic Ag is transformed mostly into silver sulfide (Kaegi et al., 2013; Ma et al., 2014) and silver bound to thiols in the sewage system. This transformation strongly affects the behavior of Ag in the environment (Levard et al., 2012; Pradas del Real et al., 2017).

Another potential environmental exposure scenario in terrestrial ecosystems is the use of Ag as a nanopesticide or nanofertilizer via the direct application of metallic Ag to agricultural soils. Ag has bactericidal, fungicidal, insecticidal and herbicidal properties, and AgNPs have high inhibitory activity against crop pathogens (Chhipa, 2019; Khan and Rizvi, 2017). Moreover, AgNPs positively impact root elongation and the general growth of cultivated plants (Chhipa, 2019) when applied at concentrations between 1 and 200 ppm, depending on the plant species. However, at these concentrations, AgNPs are toxic to a variety of organisms.

The toxicological effects of AgNPs are quite well documented and include numerous impacts on soil microflora, flora and soil invertebrates (Courtois et al., 2019). The potential transfer of Ag in plants has received more attention (Yan and Chen, 2019) than transfer of Ag in animals. Most studies in animals have focused on life traits and protein changes in exposed animals (Yu et al., 2013). Although accumulation of Ag could be an important vector of the transfer of this metal in the trophic chain, studies of the underlying mechanisms are scarce.

In soil ecotoxicology, earthworms are widely studied based on their key role in most continental ecosystems and importance in the soil macrofauna. Earthworms participate in the maintenance of soil structure and fertility. In addition to enriching the soil with organic matter available for plants, they aerate the soil and promote water penetration by forming galleries during their burrowing activity (Bernard et al., 2010; Carbonell et al., 2009). Earthworms are highly consumed by birds, snakes, insectivorous mammals and rodents, especially during tillage. Consequently, accumulated contaminants can quickly move to upper trophic levels.

82   Studying Ag accumulation/defense mechanisms requires comprehensive knowledge of Ag distribution

83   and speciation. In the present study, we investigated the accumulation, localization, and speciation of Ag

84   (presented as NM-300K AgNPs or AgNO$_3$) in earthworms using several X-ray techniques. The main objective

85   was to better understand how earthworms cope with Ag soil contamination in the context of silver

86   pesticide/fertilizer use. For this purpose, *Eisenia fetida* earthworms were exposed to artificial OECD soil

87   contaminated with a range of AgNP concentrations for 4 weeks. The effect of ionic Ag (AgNO$_3$) was

88   investigated as a positive control. Biomass and mortality were followed, and Ag accumulation, speciation and

89   localization in earthworms were measured. Finally, the accumulation mechanisms are discussed.

90

91   **2. MATERIALS AND METHODS**

92   *2.1 Test species*

93   Genetically identified *Eisenia fetida* earthworms (Homa et al., 2015) from the laboratory breeding

94   facility (LGCgE, University of Lille) were fed cow manure *ad libitum*. Adult earthworms, clitellated or not, were

95   randomly selected and introduced into the microcosms after being weighed individually. The earthworms

96   weighed 296 mg on average (min: 104 mg, max: 751 mg, mean standard deviation: 95 mg).

97

98   *2.2. Soil*

99   Artificial soil was prepared for this experiment according to OECD guideline n° 207 (OECD, 1984) and

100   contained 10% sphagnum peat moss, 20% kaolin clay and 70% quartz sand. The soil pH was adjusted with

101   calcium carbonate to 6 ± 0.5. Five weeks before adding the contaminant, 16.5 kg of soil was moistened with 6

102   liters of demineralized water. When the earthworms were added to the soil, water represented 27% of the weight

103   of the wet soil.

104

105   *2.3. Silver species*

106   The standard reference material Ag-NM300K from the European Commission Joint Research Centre

107   (JRC) was used as the AgNP source and was fully characterized in a previous work (Klein et al., 2011).

108   Commercial NM300K-NPs were kindly provided by the Fraunhofer Institute for Molecular Biology and Applied

109   Ecology IME. Each bottle contained 2 g of NM300K diluted in dispersant with a volume of 2 mL. These

110   metallic nanoparticles (NPs) were spherical and not coated and were dispersed in polyoxyethylene glycerol

111   trioleate and polyoxyethylene sorbitan mono-laurate (dispersant) with a nominal silver content of 10.2% by

weight. Ninety-nine percent of the particles had a nominal size below 20 nm. Transmission electron microscopy

indicated a mean size of 17 ± 8 nm. Smaller NPs of approximately 5 nm were also present (Mendes et al., 2015).

AgNO$_3$ solution was also prepared for comparison with exposure to Ag in ionic form. Silver nitrate salt

(AgNO$_3$) was dissolved in sterile distilled water. The AgNPs and AgNO$_3$ solution were diluted with ultrapure

water to obtain a final Ag concentration of 2 mg mL^{-1}.

2.4. Experimental scheme (earthworm exposure)

Earthworms in microcosms (with OECD artificial soil) were exposed to a range of Ag forms and

concentrations. Four types of soil mixtures corresponding to 2 controls and 2 exposed conditions were prepared:

control (soil only), dispersant (soil spiked with dispersant solution), AgNPs (soil spiked with AgNP solution) and

AgNO$_3$ (soil spiked with AgNO$_3$ solution) (see Sup. Inf 1). Four different Ag concentrations, C1, C2, C3 and

C4, were used for the AgNP and AgNO$_3$ microcosms: 30 ($\pm$ 20), 70 ($\pm$ 10), 120 ($\pm$ 15) and 280 ($\pm$ 40) mg kg^{-1}

(dry matter), respectively (these concentrations were chosen based on mortality rates reported in Garcia-Velasco

et al. (2016) and Gomes et al. (2015)). Four different volumes of NM300K dispersant were used in the dispersant

microcosms, which served as controls. These volumes were named D1, D2, D3 and D4 and corresponded to the

dispersant volumes added in the AgNP microcosms for C1, C2, C3 and C4, respectively. Thus, a total of 13

microcosm conditions were established in triplicate. Ten earthworms were introduced in each microcosm, with a

total of 390 earthworms. The exposure lasted 4 weeks. No food was added to the initial soil or during exposure.

2.5. Analyses

Life traits. Survival and biomass were measured. Biomass was followed by comparing the masses of the

groups of organisms before and after exposure, and the results were expressed as the percentage loss.

Metal concentrations in soils and accumulation in earthworms. Immediately before exposure (T0),

unexposed earthworms from the breeding facility were sacrificed to measure the metal concentrations present in

the organisms. After exposure, earthworms were collected from each microcosm and placed in 1% agar for 24

hours for depuration (i.e. to remove the gut content). Then, the earthworms were sacrificed by freezing for at

least 48 hours and freeze-dried. The organisms were reduced to powder using liquid nitrogen and mineralized by

digestion in acid medium (using HNO$_3$, H$_2$SO$_4$ and HCl$_4$ in a ratio of 10:2:3) as described by Bernard et al.

(2010).

142   Soil samples were collected at the beginning (T0) and at the end of exposure (Tf = 4 weeks). These samples were

143   freeze-dried and ground with a mortar and a pestle. For mineralization, 300 mg of sample was digested in 7 mL

144   of concentrated HNO_3 using a Berghof microwave digestion system (speed wave MWS-2 microwave pressure

145   digestion). The solutions obtained (mineralized earthworms and soils) were analyzed by ICP-OES (inductively

146   coupled plasma-optical emission spectrometry) (Varian 720-ES, USA). The following classically studied metals

147   were quantified: arsenic (As), chromium (Cr), cadmium (Cd), copper (Cu), nickel (Ni), lead (Pb), zinc (Zn) and

148   Ag.

149

150   *Localization of silver in exposed earthworms using X-ray 3D imaging*

151   Two earthworms were imaged in 3D using X-ray micro-computed tomography (micro-CT): one non-exposed

152   sample and one sample exposed to AgNPs (AgNP-C3) collected after 4 weeks in the dispersant and AgNP

153   microcosms, respectively.

154   *Sample preparation*. After 24 hours of depuration in 1% agar, the earthworms were first anesthetized on ice and

155   fixed for 16 hours in ice-cold 4% paraformaldehyde in 0.1 M phosphate buffer. They were then dehydrated by

156   soaking in a graded series of ethanol solutions (from 30% vol to 100% vol.) and subjected to supercritical point

157   drying (Leica EM CPD300°). In this drying process, ethanol is replaced with liquid CO_2, which avoids the

158   creation of damaging surface tension forces associated with drying by bringing the liquid in the sample to the gas

159   phase without crossing the liquid-gas phase boundary. The dried samples were finally placed in polyimide tubing

160   (Kapton).

161   *3D image acquisition.* 3D imaging of the earthworms was performed with a microXCT-400 X-ray microscope

162   (Zeiss). High-resolution scans were acquired at 40 kV and 250 µA. A total of 2501 projections were collected

163   through 360° rotation with an exposure time of 20 s per projection. A 20x magnification optical objective was

164   selected to achieved an isotropic voxel of 0.9 µm and a field-of-view (FOV) of 0.9x0.9x0.9 mm^3. The FOV was

165   centered at the lower end of the earthworm (rings 9 and 10 for the control and exposed earthworms, respectively)

166   and included the coelomic cavity and the nephridia epithelium. The position of the FOV was selected from pre-

167   visualization scans of the entire earthworm with lower spatial resolution (Supporting information 2). Volume

168   reconstruction was performed with XMReconstructed-Parallel Beam-9.0.6445 software using a filtered back

169   projection algorithm.

170   *3D image analysis.* Avizo 8.0 software (Hillsboro, OR, USA) was used for the visualization, processing, and

171   analysis of the reconstructed dataset. The procedure developed in Chaurand et al. (2018) to isolate metal-based

NPs was followed. Briefly, images of exposed and non-exposed (control) samples were compared after histogram x-axis normalization (i.e. colormap normalization). The histogram represents the X-ray attenuation in each voxel (expressed as an arbitrary gray scale value, GSV) of the analyzed volume as a function of the number of voxels for each GSV (intensity). The histogram x-axis was normalized using air as an internal standard. After the normalization step, the brilliant voxels in the image of the exposed sample that were not identified in the image of the control sample were attributed to the presence of Ag by thresholding (Supporting information 3).

Speciation of silver in soils and earthworms. Silver speciation in soil and earthworms was determined by X-ray absorption near-edge structure (XANES) spectroscopy, which permits the determination of the local atomic environment (speciation) of targeted atoms present in complex media. Silver K-edge (25.51 keV) XANES spectra were acquired at the European Synchrotron Radiation Facility (ESRF, France) on the FAME beamline (BM30b) with Si(220) monochromator crystals (Proux et al., 2005). Prior to analysis, the earthworm samples were lyophilized, ground and pressed into 5-mm pellets. Spectral acquisition was performed at liquid helium temperature to avoid sample evolution under the beam. Measurements were carried out in fluorescence mode using a 30-element Canberra Ge solid-state detector. Each spectrum was the sum of at least three scans. A set of model compounds including metallic AgNPs, $AgNO_3$, Ag_2S, AgCl, Ag-thiocarbamate (Ag-thio), and Ag-humic acid (Ag-HA) was run in transmission mode. Normalization data reduction and linear combination fitting (LCF) were performed according to standard methods using Athena software (Ravel and Newville, 2005). The residual factor of LCF was calculated according to the formula $R = \sum(\exp - \mathrm{fit})^2 / \sum(\exp)^2$, where the sums are over the data points in the fitting region. At each step of the fitting, an additional reference spectrum was added if the following two conditions were true: the R factor decreased by 20% or more and the additional reference had a contribution equal to or higher than 10% among Ag species.

2.6. Statistical analysis

For biomass, mortality and metal content in earthworms, the majority of the data did not follow a normal distribution, and the variances were not homogeneous (Shapiro, Liliefors and Bartlett tests). Thus, Sheirer-Ray-Hare non-parametric tests and post-hoc tests based on ranks were used. For data following a normal distribution with homogeneous variances, ANOVA tests and Tuckey post-hoc tests were used. Correlation matrices (based on the Kendall method) were constructed. Tests were performed using the R package (R Core Team, 2018).

202

3. RESULTS

Metal quantities in soil. At the initial time point, the concentrations of As, Cr, Cu, Ni, Pb and Zn were 1.08 (standard deviation 0.34), 1.05 (s.d. 0.30), 5.31 (s.d. 1.22), 0.62 (s.d. 0.38), 10.13 (s.d. 2.11) and 5.16 (s.d. 0.66) mg kg^{-1}, respectively. The concentration of Cd was below the detection limit. The Ag concentrations in the microcosms are shown in Table 1. As expected, there was no significant difference in Ag doses between the AgNP and AgNO$_3$ microcosms at each concentration (C1, C2, C3 and C4). Only very low concentrations of Ag were detected in the control and dispersant microcosms. One control microcosm appeared to have been very slightly contaminated by accident, but its Ag concentration remained negligible compared with the exposure conditions.

The concentrations of other metals were very low compared with Ag, which suggests that these metals would not hinder the accumulation of Ag by earthworms.

Life traits. A survival rate of 100% was observed in all of the control, dispersant and AgNP microcosms (Fig. 1). In the AgNO$_3$ microcosms, dose-dependent mortality was observed, with 6.7% mortality at the lowest concentration and 100% mortality at the highest concentration. During the 4 weeks of exposure, the earthworms lost weight in all microcosms, including the controls. Thus, the loss of weight cannot be linked to Ag contamination. Biomass data for earthworms in the AgNO$_3$-C4 microcosm are absent due to total mortality.

Metals bioaccumulation: silver. At the end of exposure, the Ag content in earthworms varied among the different treatments (Fig. 2). Silver was not detected in organisms in the control microcosms. In the presence of Ag, earthworms accumulated between 2.8 and 9.9 mg kg^{-1} (average 5 mg kg^{-1} of dry matter). The accumulation of Ag in the earthworms exposed to Ag was independent of the form of Ag (NPs or ionic) or the Ag dose in the microcosm. Data for earthworms in the AgNO3-C3 and AgNO3-C4 microcosms are absent because the insufficient quantity of material available for analysis due to significant mortality.

Metals bioaccumulation: other metals. No significant variations of metal quantities in earthworm bodies were observed for Cd, Cr, Ni, Pb and Zn compared with the corresponding control. A single significant difference in As concentration was observed between the AgNO$_3$-C2 microcosm and its control (Supporting information 2). The Cu concentration in earthworms was similar in all treatments without Ag (Fig. 3). In the

232 AgNO$_3$-C2 microcosm (no results were obtained for the AgNO$_3$-C3 and AgNO$_3$-C4 microcosms because of

233 earthworm mortality), there was a decrease in the Cu concentration, but this difference was not significant

234 compared with the control. However, in the AgNP microcosms, earthworms accumulated significantly less Cu

235 (approximately two times less) compared with the controls.

236 In summary, Ag was the only metal present in greater concentrations in earthworms exposed to AgNPs

237 conditions than in those under control conditions.

238

239 *Localization of Ag in earthworms:* Brilliant voxels (i.e. voxels exhibiting high X-ray absorption) were

240 observed in the micro-CT volume of exposed earthworms (AgNP-C3, with 109.57 (± 8.05) mg kg^{-1} of AgNPs).

241 Although this imaging technique cannot identify the source of these brilliant voxels, they were not observed in

242 the non-exposed earthworm volume (Dis-D3, in dispersant) and can therefore be attributed to Ag accumulation

243 areas by thresholding (Fig. 4) due to the absence of differences in bioaccumulation for other elements with high

244 densities (metals). Thresholding provides the distribution of these areas of brilliant voxels (colored in red) in the

245 whole scanned volume. Ag accumulation areas/spots were observed around the digestive tract, in the coelomic

246 cavity, in free cells in the coelomic cavity (coelomocytes) and in the nephridial epithelium (Fig. 4).

247

248 *Speciation of silver.* Ag speciation in OECD soil after 4 weeks of incubation depended on the initial

249 form (NPs or ionic). Ag initially spiked as AgNPs remained mainly metallic, but approximately 15% became

250 complexed with natural organic thiols (Fig. 5). Ag initially spiked as AgNO$_3$ was linked with humic acid (52%)

251 and organic thiols (33%), and approximately 15% was in metallic form. Regardless of the exposure scenario

252 (AgNPs or AgNO$_3$), the speciation of Ag accumulated in earthworms was similar and consisted of Ag bound to

253 thiols (Fig. 5).

254

255

256 **4. DISCUSSION**

257

258 OECD soil is a simplified matrix for evaluating the effects of medium- and long-term exposure in a soil

259 naturally deprived of many metals and other contaminants. In the present study, the use of OECD soil allowed

260 the effects of added Ag and the underlying mechanisms to be explored under simplified experimental conditions.

261 To prevent the possible ingestion of additional metals, no food was added to the medium. Use of this medium

was therefore appropriate for the main objective of our work, which was to locate the sites of Ag accumulation by micro-CT.

High AgNP concentrations did not affect the life traits of *E. fetida* earthworms. The weight loss observed in the AgNPs microcosms was similar to that observed under control conditions and was due to a lack of food. OECD soil is poor in organic matter and nutrients, and food was not provided during the experiment. By contrast, dose-dependent toxicity of $AgNO_3$ resulting in weight loss and mortality was observed. Thus, the toxicity of Ag^+ was stronger than that of AgNPs, consistent with previous observations of *E. fetida* in both artificial (Diez-Ortiz et al., 2015a; Gomes et al., 2015; Heckmann et al., 2011) and natural soils (Novo et al., 2015). Higher toxicity of ionic Ag compared with AgNPs has been reported for many plants and animal species (Courtois et al., 2019), and there is a consensus that the toxicity of Ag is mainly due to its ionic form. We recognize that the starvation of the earthworms may have interfered with the results presented here. In the presence of optimal food, the effects of the two forms of Ag might be exacerbated or reduced.

Despite the differences in toxicity observed between the treatments, in all conditions with Ag (ionic or NPs), the mean bioaccumulation by earthworms in the body was 4 to 5 mg kg^{-1} (dry matter). Thus, the form of Ag (NPs or ionic) had no influence on the amount of Ag bioaccumulation. In earthworms, metal accumulation is related not only to food intake but also to dermal absorption of dissolved ions (Vijver et al., 2003). Because of the differences in Ag speciation in soil, one might expect Ag linked to organic matter (humic acids) to be metabolized more readily than thiolated Ag. When combined with the dermal absorption of Ag^+ ions, this increased metabolism could explain the higher toxicity of $AgNO_3$. However, (Diez-Ortiz et al., 2015b; Garcia-Velasco et al., 2016) showed that Ag is mainly internalized by soil ingestion. Our bioaccumulation results show that Ag can enter the earthworm body. Ag may also pass though the epidermis as dissolved Ag^+ ions. Unrine et al. (2008) demonstrated that dermal absorption of Au nanoparticles occurs in earthworms. However, as mentioned previously, dermal absorption is not the main route of metal internalization.

Contradictory results were reported by Shoults-Wilson et al. (2010) and Bourdineaud et al. (2019), who showed that *E. fetida* in artificial soil accumulated two to fifteen times more silver when exposed to $AgNO_3$ compared with AgNPs. Interestingly, these authors used AgNPs that were two to three times larger (between 50 and 60 nm) than the NM-300K AgNPs used in this study, which may have hindered the dermal absorption and metabolism of AgNPs. Supporting this hypothesis, Unrine et al. (2008) showed that the internalization of metallic NPs (Zn and Au) in *E. fetida* decreased with increasing NP size.

291   The Ag concentration in the soil did not influence Ag bioaccumulation by earthworms, which suggests

292   that a very efficient regulation mechanism limits the internal content of Ag even when the environmental

293   concentration is very high. A similar phenomenon (plateau and regulation) was reported by Coutris et al. (2011),

294   who observed rapid Ag excretion from *E. fetida* after the end of exposure.

295   Regardless of the original form of Ag in the microcosms, the bioaccumulated Ag in earthworms was

296   always bound to organic thiols. However, in OECD soil, even after 4 weeks of incubation, Ag speciation differed

297   greatly between the AgNP and $AgNO_3$ microcosms, indicating biotransformation of Ag by earthworms. Since a

298   regulation/excretion mechanism limits the Ag content in the body, it is likely that earthworms release Ag after

299   biotransformation. Thus, soil organisms like earthworms might change the speciation of Ag in the environment

300   and, consequently, its availability.

301   3D images of entire earthworms obtained by micro-CT showed that Ag (originating from AgNPs) was

302   stored and/or transiting in chloragogenous tissue, coelomocytes and the nephridial epithelium. A similar result

303   was obtained by Diez-Ortiz et al. (2015b) by X-ray chemical analysis (micro-XRF) of the internal distribution in

304   transverse sections: Ag was observed in the gut wall, liver-like chloragogenous tissue and nephridia. These cells

305   and organs are related to immunity and detoxification functions. Chloragogenous tissue covers the outer part of

306   the intestine and is considered to have a liver-like function. For instance, the chloragogenous tissue accumulates

307   wastes produced by digestion and can sequester metals (Lapied et al., 2010; Morgan and Morgan, 1993; Vijver

308   et al., 2004). Moreover, chloragogenous tissue plays a role in earthworm immunity (Fischer, 1993).

309   Coelomocytes are immune cells involved in the elimination of foreign bodies by phagocytosis and encapsulation

310   (Garcia-Velasco et al., 2017), and at least some coelomocytes are derived from chloragocytes (Hamed et al.,

311   2002). Nephridia are organs involved in osmoregulation and excretion (Davidson et al., 2013).

312   In the present study, accumulation of Ag was concomitant with a decrease in Cu accumulation. Cu is an

313   essential metal that is specifically stored by metallothioneins (MTs). MTs, stress proteins that bind essential and

314   non-essential metals through thiolated bonds, participate in the homeostasis of essential metals such as Zn and

315   Cu as well as non-essential metals such as Cd or mercury (Hg) (Demuynck et al., 2006; Vijver et al., 2004).

316   Interestingly, in earthworms, MTs are preferentially but not exclusively localized in the epithelial cells of the

317   intestine, chloragogenous tissue, coelomocytes and nephridia (Morgan et al., 2004). According to the

318   localization of Ag observed by micro-CT, its internal speciation (linked to a thiolated molecule), and competition

319   with Cu, Ag is probably bound by MTs in earthworms. The same hypothesis was proposed by Baccaro et al.

320   (2018), who also observed that bioaccumulated Ag was related to sulfur. Furthermore, in mice, Ag can bind to

321 MT with higher affinity than Cu (Sugawara and Sugawara, 1984). Consequently, Ag probably displaces Cu from

322 MT. Moreover, Hayashi et al. (2013) and Curieses Silvana et al. (2017) observed changes in the expression of

323 genes encoding MTs in *E. fetida* exposed to AgNPs and $AgNO_3$ (in natural and OECD soil, respectively).

324 Therefore, it seems that MTs have a role in the detoxification mechanisms of Ag. Taken together, these results

325 suggest a pathway for the absorption, detoxification and excretion of Ag.

326   In summary, Ag is probably mainly taken up by ingestion, absorbed by the gut and at least temporarily

327 stored in chloragogenous tissue before detoxification. For excretion, Ag must be transferred from chloragocytes

328 to the nephridia. Two mechanisms can be proposed. First, MT-metal complexes are discharged from the

329 coelomic cavity and then excreted by the nephridia. This mechanism is supported by the work of Nordberg

330 (1989) and Morgan et al. (2004), who described the capacity of MTs linked to metals to enter excretory organs in

331 mammals and earthworms. Second, Ag could be transferred to coelomocytes in the coelomic cavity and stored,

332 inducing the gene encoding MTII (Brulle et al., 2008). Transfer of Ag into coelomocytes can occur via two

333 pathways: transformation of chloragocytes that have stored Ag into free coelomocyte cells or release of metal-

334 bound MT into the coelomic cavity by chloragocytes and subsequent uptake by coelomocytes. In the event of

335 excessive ingestion of Ag that can be not managed conventionally by storage in proteins and excretion, another

336 mechanism might help limit the levels of Ag in the body. For example, Roubalová et al. (2018) showed that

337 when earthworms are confronted by aggression, earthworms can expel coelomic fluid with coelomocytes via the

338 dorsal pores. This mechanism would quickly remove from the body a large amount of metals trapped in the

339 coelomocytes.

340

342

343   *Table 1: Silver content in the microcosms at the initial time point (mean in mg kg^{-1} of dry matter). The results*

344   *were obtained by ICP analysis. Standard deviations are in parentheses.*

345   *Figure 1: A. Mean percentage of weight loss of the earthworm groups in the microcosms between the beginning*

346   *and end of the experiment. B. Mean percentage of earthworm survival in the microcosms between the beginning*

347   *and end of the experiment. The concentrations C1, C2, C3 and C4 correspond to mean concentrations of AgNO$_3$*

348   *and AgNPs of 33 (± 16), 71 (± 8), 117 (± 11) and 277 (± 24) mg kg^{-1} (dry matter) (the values were not*

349   *significantly different between the two Ag sources). Asterisks (*) indicate statistically important differences*

350   *between the Ag treatment and control. Lowercase letters in green indicate significant differences in biomass*

351   *between the 4 doses of Ag (for one form of Ag). Lowercase letters in blue indicate significant differences in*

352   *survival between the 4 doses of Ag (for one form of Ag). Uppercase letters in yellow indicate significant*

353   *differences in biomass between the two forms of Ag (NPs or ionic), taking into account all concentrations. 'NA'*

354   *indicates that biomass data were not available due to total mortality.*

355   *Figure 2: Ag content in earthworm bodies (mg kg^{-1}). "AgNPs" corresponds to microcosms with silver*

356   *nanoparticles. "AgNO$_3$" corresponds to microcosms with silver nitrate. The concentrations C1, C2, C3 and C4*

357   *correspond to 33 (± 16), 71 (± 8), 117 (± 11) and 277 (± 24) mg kg^{-1} (dry matter) (the mean concentrations of*

358   *AgNO$_3$ and AgNPs were not significantly different). Stars (*) indicate significant differences from the associated*

359   *control without silver. Lowercase letters in orange indicate significant differences in metal content between the 4*

360   *concentrations (C1, C2, C3 and C4) of Ag (AgNPs and AgNO$_3$ were not compared). Uppercase letters in yellow*

361   *indicate significant differences in Ag content between the 2 forms of Ag (NPs or ionic), taking into account all*

362   *concentrations. 'NA' indicates that data were not available due to significant mortality.*

363   *Figure 3: Cu contents in earthworm bodies (mg kg^{-1}). "AgNPs" corresponds to microcosms with silver*

364   *nanoparticles. "AgNO$_3$" corresponds to microcosms with silver nitrate. The concentrations C1, C2, C3 and C4*

365   *correspond to 33 (± 16), 71 (± 8), 117 (± 11) and 277 (± 24) mg kg^{-1} (dry matter) (mean concentrations of*

366   *AgNO$_3$ and AgNPs, which were not significantly different). Stars (*) indicate significant differences from the*

367   *associated control without Ag. Lowercase letters in purple indicate significant differences in metal contents*

368   *among the 4 doses of Ag (for one form of Ag). Uppercase letters in yellow indicate significant differences in Cu*

369   *content between the 2 forms of Ag (NPs or ionic), taking into account all concentrations. Lowercase letters in*

370 *black indicate significant differences in Cu content between the 2 forms of Ag at one given concentration. 'NA'*

371 *indicates that data were not available due to significant mortality.*

372 *Figure 4: Examples of 2D orthoslices extracted from the reconstructed volume of (A) non-exposed earthworms*

373 *(Dis-D3) and (B, C, D) exposed earthworms (AgNP-C3). The digestive tract (d), free cells in the coelomic cavity*

374 *(coelomocytes) (c) and the nephridial epithelium (n) are indicated. The pixels colored in red in (B, C, D) in*

375 *dotted circles are brilliant voxels isolated by thresholding and associated with Ag. These brilliant pixels are not*

376 *observed in (A). 1 px = 0.9 μm.*

377 *Figure 5: A. Linear combination fitting (LCF) of the XANES spectra of the samples collected at different time*

378 *points (dotted lines) and experimental spectra (solid lines) of soil and earthworms after 4 weeks of exposure to*

379 *AgNPs and AgNO$_3$. The curves for the samples are colored as follows: dark green, soil spiked with AgNO$_3$; dark*

380 *blue, soil spiked with AgNPs; light green, earthworms exposed to AgNO$_3$; light blue, earthworms exposed to*

381 *AgNPs. B. XANES spectra of the model compounds used for LCF. Ag-HA (in yellow) was used as a proxy for Ag*

382 *complexed to natural organic matter (humic acids). AgNPs (in grey) corresponds to the initial NM300K AgNPs*

383 *used for the experiment. Ag-thiol (in purple) was used as a proxy for Ag bound to an organic thiol. Ag$_2$S (in*

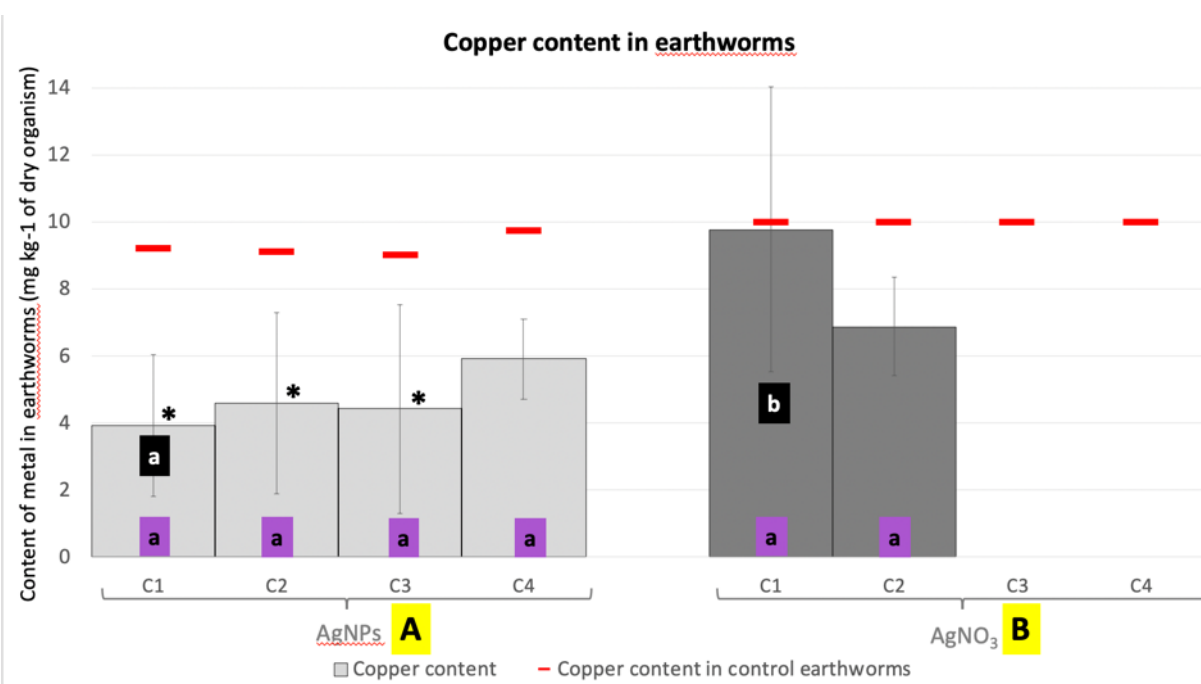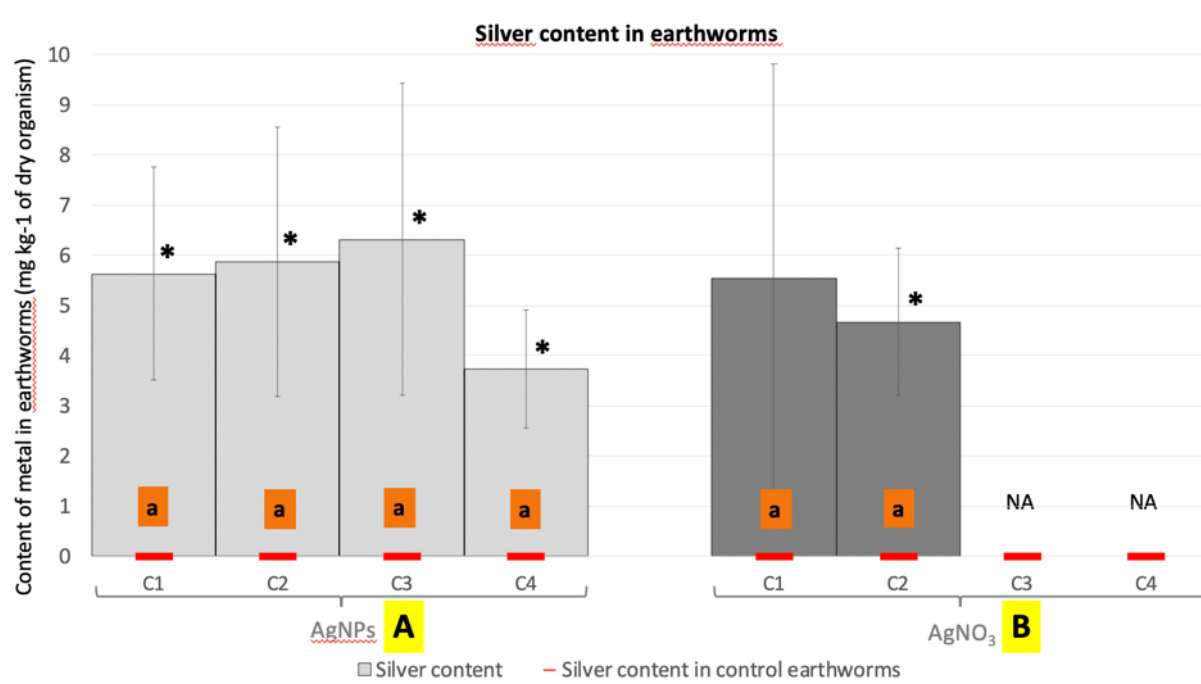384 *orange) corresponds to silver sulfide (acanthite mineral).*

385 *Sup. Inf. 1: Scheme of the experimental design. "Control" corresponds to the microcosm without any inputs.*

386 *"AgNPs" corresponds to silver nanoparticles. "Dis" corresponds to dispersant. "AgNO$_3$" corresponds to silver*

387 *nitrate. The concentrations C1, C2, C3 and C4 correspond to 33 (± 16), 71 (± 8), 117 (± 11) and 277 (± 24) mg*

388 *kg^{-1} of Ag (dry matter) (the mean concentrations of AgNO$_3$ and AgNPs were not significantly different). The*

389 *volumes D1, D2, D3 and D4 correspond to the volumes of dispersant added to the microcosms. Dispersant was*

390 *added in the same amount as in the corresponding AgNPs microcosms, that is, 1.599, 2.666, 5.331 and 10.662*
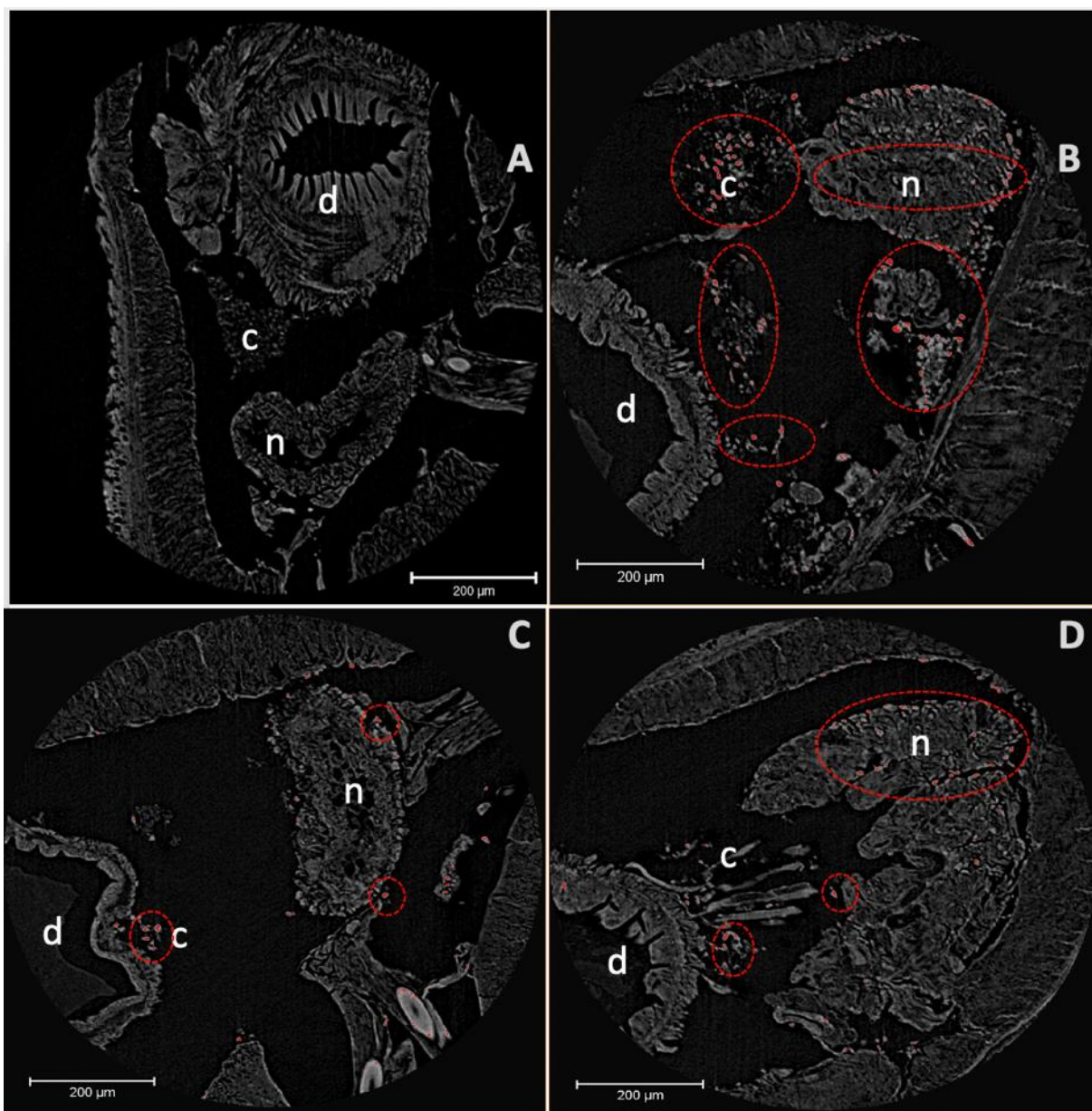
391 *mL.*

392 *Sup. Inf. 2: Metal contents in earthworms (mean in mg kg^{-1}). The results were obtained by ICP analysis.*

393 *"Control" corresponds to the microcosm without silver addition. "AgNPs" corresponds to silver nanoparticles.*

394 *"Dis" corresponds to dispersant. "AgNO$_3$" corresponds to silver nitrate. The concentrations C1, C2, C3 and C4*

395 *correspond to 33 (± 20), 71 (± 10), 117 (± 15) and 277 (± 45) mg kg^{-1} (dry matter) (the mean concentrations of*

396 *AgNO$_3$ and AgNPs were not significantly different). Stars (*) indicate significant differences between the*

397 *condition with Ag and the associated control without Ag. Standard deviations are in parentheses.*

398 *Sup. Inf. 3: 3D imaging of an earthworm by micro-CT. (top) Selection of FOV for high-resolution micro-CT*

399 *scan. (bottom) 3D image analysis procedure for isolating Ag accumulation areas (normalization and*

400 *thresholding step).*

Concentration	Control microcosms	Dispersant	AgNPs	AgNO$_3$
C1 (or D1)		0.69 (0.97)	26.33 (10.63)	39.53 (20.66)
C2 (or D2)	1.95 (1.23)	0.61 (1.06)	70.50 (8.15)	71.03 (8.71)
C3 (or D3)		0.18 (0.31)	109.57 (8.05)	124.30 (7.59)
C4 (or D4)		0.00 (0.00)	262.93 (27.87)	290.90 (10.81)

401

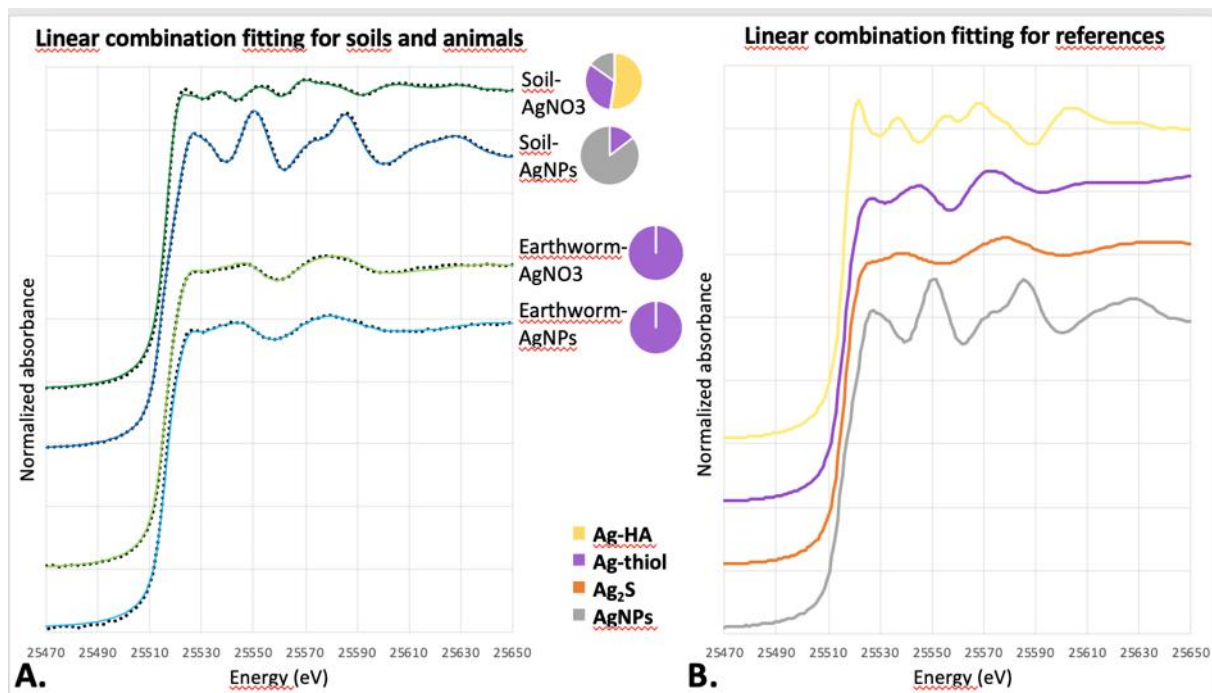402 A   B

403

15

Silver content in earthworms

404

405

Copper content in earthworms

406

407

16
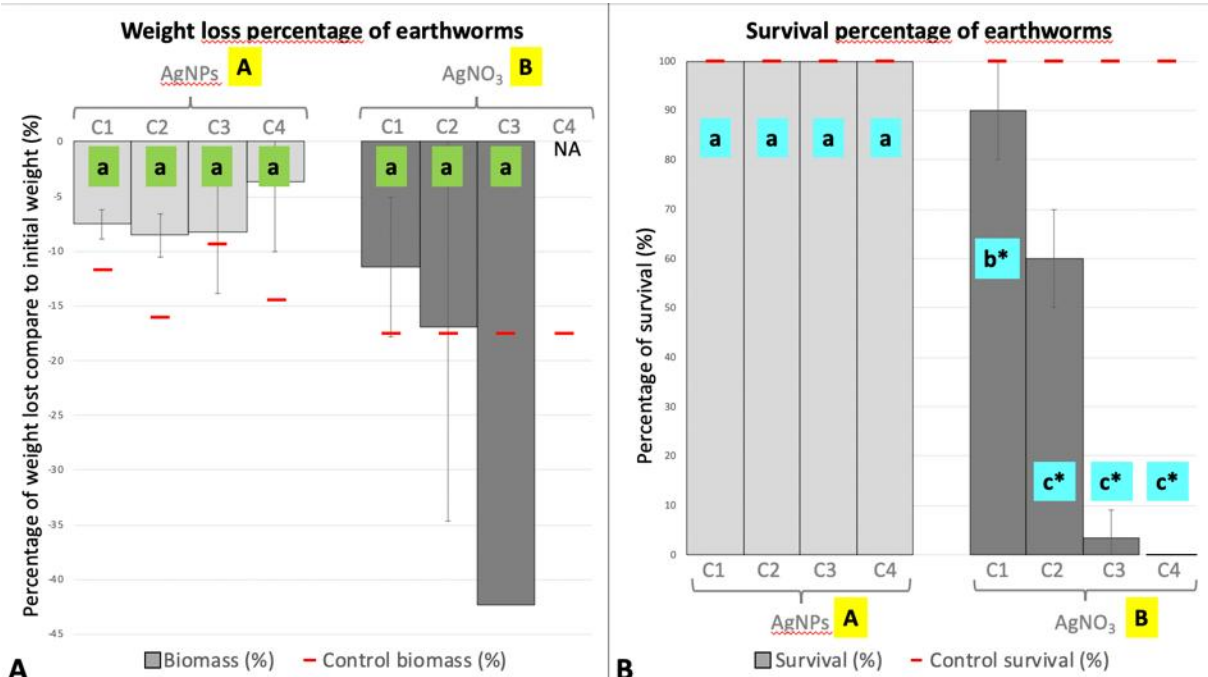
low   X-ray absorption   high

408

409

Linear combination fitting for soils and animals

Linear combination fitting for references

Soil-AgNO3
Soil-AgNPs
Earthworm-AgNO3
Earthworm-AgNPs

Ag-HA
Ag-thiol
Ag₂S
AgNPs

410
411

References

Baccaro, M., Undas, A.K., de Vriendt, J., van den Berg, J.H.J., Peters, R.J.B., van den Brink, N.W., 2018. Ageing, dissolution and biogenic formation of nanoparticles: how do these factors affect the uptake kinetics of silver nanoparticles in earthworms? Environ. Sci. Nano 5, 1107–1116. https://doi.org/10.1039/C7EN01212H

Bernard, F., Brulle, F., Douay, F., Lemière, S., Demuynck, S., Vandenbulcke, F., 2010. Metallic trace element body burdens and gene expression analysis of biomarker candidates in Eisenia fetida, using an "exposure/depuration" experimental scheme with field soils. Ecotoxicol. Environ. Saf. 73, 1034–1045. https://doi.org/10.1016/j.ecoenv.2010.01.010

Bourdineaud, J.-P., Štambuk, A., Šrut, M., Radić Brkanac, S., Ivanković, D., Lisjak, D., Sauerborn Klobučar, R., Dragun, Z., Bačić, N., Klobučar, G.I.V., 2019. Gold and silver nanoparticles effects to the earthworm *Eisenia fetida* – the importance of tissue over soil concentrations. Drug Chem. Toxicol. 1–18. https://doi.org/10.1080/01480545.2019.1567757

Brulle, F., Cocquerelle, C., Wamalah, A.N., Morgan, A.J., Kille, P., Leprêtre, A., Vandenbulcke, F., 2008. cDNA cloning and expression analysis of Eisenia fetida (Annelida: Oligochaeta) phytochelatin synthase under cadmium exposure. Ecotoxicol. Environ. Saf. 71, 47–55. https://doi.org/10.1016/j.ecoenv.2007.10.032

Carbonell, G., Pro, J., Gómez, N., Babín, M.M., Fernández, C., Alonso, E., Tarazona, J.V., 2009. Sewage sludge applied to agricultural soil: Ecotoxicological effects on representative soil organisms. Ecotoxicol. Environ. Saf. 72, 1309–1319. https://doi.org/10.1016/j.ecoenv.2009.01.007

Chaurand, P., Liu, W., Borschneck, D., Levard, C., Auffan, M., Paul, E., Collin, B., Kieffer, I., Lanone, S., Rose, J., Perrin, J., 2018. Multi-scale X-ray computed tomography to detect and localize metal-based nanomaterials in lung tissues of in vivo exposed mice. Sci. Rep. 8, 1–11. https://doi.org/10.1038/s41598-018-21862-4

Chhipa, H., 2019. Applications of nanotechnology in agriculture. Methods Microbiol. 115–142.

Courtois, P., Rorat, A., Lemiere, S., Guyoneaud, R., Attard, E., Levard, C., Vandenbulcke, F., 2019. Ecotoxicology of silver nanoparticles and their derivatives introduced in soil with or without sewage sludge: A review of effects on microorganisms, plants and animals. Environ. Pollut. 253, 578–598. https://doi.org/10.1016/j.envpol.2019.07.053

Coutris, C., Hertel-Aas, T., Lapied, E., Joner, E.J., Oughton, D.H., 2011. Bioavailability of cobalt and silver nanoparticles to the earthworm Eisenia fetida. Nanotoxicology 6, 186–195. https://doi.org/10.3109/17435390.2011.569094

Curieses Silvana, P., García-Velasco, N., Urionabarrenetxea, E., Elena, S.M., Bilbao, E., Di Marzio Walter, D., Soto, M., 2017. Responses to silver nanoparticles and silver nitrate in a battery of biomarkers measured in coelomocytes and in target tissues of Eisenia fetida earthworms. Ecotoxicol. Environ. Saf. 141, 57–63. https://doi.org/10.1016/j.ecoenv.2017.03.008

Davidson, S.K., Powell, R., James, S., 2013. A global survey of the bacteria within earthworm nephridia. Mol. Phylogenet. Evol. 67, 188–200. https://doi.org/10.1016/j.ympev.2012.12.005

Demuynck, S., Grumiaux, F., Mottier, V., Schikorski, D., Lemière, S., Leprêtre, A., 2006. Metallothionein response following cadmium exposure in the oligochaete Eisenia fetida. Comp. Biochem. Physiol. Toxicol. Pharmacol. CBP 144, 34–46. https://doi.org/10.1016/j.cbpc.2006.05.004

Diez-Ortiz, M., Lahive, E., George, S., Ter Schure, A., Van Gestel, C.A.M., Jurkschat, K., Svendsen, C., Spurgeon, D.J., 2015a. Short-term soil bioassays may not reveal the full toxicity potential for nanomaterials; bioavailability and toxicity of silver ions (AgNO3) and silver nanoparticles to earthworm Eisenia fetida in long-term aged soils. Environ. Pollut. 203, 191–198. https://doi.org/10.1016/j.envpol.2015.03.033

Diez-Ortiz, M., Lahive, E., Kille, P., Powell, K., Morgan, A.J., Jurkschat, K., Van Gestel, C.A.M., Mosselmans, J.F.W., Svendsen, C., Spurgeon, D.J., 2015b. Uptake routes and toxicokinetics of silver nanoparticles and silver ions in the earthworm Lumbricus rubellus. Environ. Toxicol. Chem. 34, 2263–2270. https://doi.org/10.1002/etc.3036

Fischer, E., 1993. The myelo-erythroid nature of the chloragogenous-like tissues of the annelids. Comp. Biochem. Physiol. A Physiol. 106, 449–453. https://doi.org/10.1016/0300-9629(93)90237-X

Garcia-Velasco, N., Gandariasbeitia, M., Irizar, A., Soto, M., 2016. Uptake route and resulting toxicity of silver nanoparticles in Eisenia fetida earthworm exposed through Standard OECD Tests. Ecotoxicology 25, 1543–1555. https://doi.org/10.1007/s10646-016-1710-2

Garcia-Velasco, N., Peña-Cearra, A., Bilbao, E., Zaldibar, B., Soto, M., 2017. Integrative assessment of the effects produced by Ag nanoparticles at different levels of biological complexity in Eisenia fetida maintained in two standard soils (OECD and LUFA 2.3). Chemosphere 181, 747–758. https://doi.org/10.1016/j.chemosphere.2017.04.143

Gomes, S.I.L., Hansen, D., Scott-Fordsmand, J.J., Amorim, M.J.B., 2015. Effects of silver nanoparticles to soil invertebrates: Oxidative stress biomarkers in Eisenia fetida. Environ. Pollut. 199, 49–55. https://doi.org/10.1016/j.envpol.2015.01.012

Hamed, S.S., Kauschke, E., Cooper, E.L., 2002. Cytochemical Properties of Earthworm Coelomocytes Enriched by Percoll, in: A New Model for Analyzing Antimicrobial Peptides with Biomedical Applications., NATO Science Series. https://doi.org/10.3923/ijzr.2005.74.83

Hayashi, Y., Heckmann, L.-H., Simonsen, V., Scott-Fordsmand, J.J., 2013. Time-course profiling of molecular stress responses to silver nanoparticles in the earthworm Eisenia fetida. Ecotoxicol. Environ. Saf. 98, 219–226. https://doi.org/10.1016/j.ecoenv.2013.08.017

Heckmann, L.-H., Hovgaard, M.B., Sutherland, D.S., Autrup, H., Besenbacher, F., Scott-Fordsmand, J.J., 2011. Limit-test toxicity screening of selected inorganic nanoparticles to the earthworm Eisenia fetida. Ecotoxicology 20, 226–233. https://doi.org/10.1007/s10646-010-0574-0

Homa, J., Rorat, A., Kruk, J., Cocquerelle, C., Plytycz, B., Vandenbulcke, F., 2015. Dermal exposure of Eisenia andrei earthworms: Effects of heavy metals on metallothionein and phytochelatin synthase gene expressions in coelomocytes. Environ. Toxicol. Chem. 34, 1397–1404. https://doi.org/10.1002/etc.2944

Kaegi, R., Voegelin, A., Ort, C., Sinnet, B., Thalmann, B., Krismer, J., Hagendorfer, H., Elumelu, M., Mueller, E., 2013. Fate and transformation of silver nanoparticles in urban wastewater systems. Water Res. 47, 3866–3877. https://doi.org/10.1016/j.watres.2012.11.060

Kaegi, R., Voegelin, A., Sinnet, B., Zuleeg, S., Hagendorfer, H., Burkhardt, M., Siegrist, H., 2011. Behavior of Metallic Silver Nanoparticles in a Pilot Wastewater Treatment Plant. Environ. Sci. Technol. 45, 3902–3908. https://doi.org/10.1021/es1041892

Khan, M.R., Rizvi, T.F., 2017. Application of Nanofertilizer and Nanopesticides for Improvements in Crop Production and Protection, in: Ghorbanpour, M., Manika, K., Varma, A. (Eds.), Nanoscience and Plant–Soil Systems, Soil Biology. Springer International Publishing, Cham, pp. 405–427. https://doi.org/10.1007/978-3-319-46835-8_15

Klein, C.L., Stahlmecke, B., Romazanov, J., Kuhlbusch, T.A.J., Van Doren, E., De Temmerman, P.-J., Mast, J., Wick, P., Krug, H., Locoro, G., Hund-Rinke, K., Kördel, W., Friedrichs, S., Maier, G., Werner, J., Linsinger, T., Gawlik, B.M., Comero, S., Institute for Health and Consumer Protection, European Commission, Joint Research Centre, Institute for Environment and Sustainability, Institute for Reference Materials and Measurements, 2011. NM-Series of representative manufactured nanomaterials: NM-300 silver characterisation, stability, homogeneity. Publications Office, Luxembourg.

Lapied, E., Moudilou, E., Exbrayat, J.-M., Oughton, D.H., Joner, E.J., 2010. Silver nanoparticle exposure causes apoptotic response in the earthworm Lumbricus terrestris (Oligochaeta). Nanomed. 5, 975–984. https://doi.org/10.2217/nnm.10.58

Levard, C., Hotze, E.M., Lowry, G.V., Brown, G.E., 2012. Environmental Transformations of Silver Nanoparticles: Impact on Stability and Toxicity. Environ. Sci. Technol. 46, 6900–6914. https://doi.org/10.1021/es2037405

Ma, R., Levard, C., Judy, J.D., Unrine, J.M., Durenkamp, M., Martin, B., Jefferson, B., Lowry, G.V., 2014. Fate of Zinc Oxide and Silver Nanoparticles in a Pilot Wastewater Treatment Plant and in Processed Biosolids. Environ. Sci. Technol. 48, 104–112. https://doi.org/10.1021/es403646x

McGillicuddy, E., Murray, I., Kavanagh, S., Morrison, L., Fogarty, A., Cormican, M., Dockery, P., Prendergast, M., Rowan, N., Morris, D., 2017. Silver nanoparticles in the environment: Sources, detection and ecotoxicology. Sci. Total Environ. 575, 231–246. https://doi.org/10.1016/j.scitotenv.2016.10.041

Mendes, L.A., Maria, V.L., Scott-Fordsmand, J.J., Amorim, M.J.B., 2015. Ag Nanoparticles (Ag NM300K) in the Terrestrial Environment: Effects at Population and Cellular Level in Folsomia candida (Collembola). Int. J. Environ. Res. Public. Health 12, 12530–12542. https://doi.org/10.3390/ijerph121012530

Morgan, A.J., Stürzenbaum, S.R., Winters, C., Grime, G.W., Aziz, N.A.A., Kille, P., 2004. Differential metallothionein expression in earthworm (Lumbricus rubellus) tissues. Ecotoxicol. Environ. Saf. 57, 11–19. https://doi.org/10.1016/j.ecoenv.2003.08.022

Morgan, J.E., Morgan, A.J., 1993. Seasonal changes in the tissue-metal (Cd, Zn and Pb) concentrations in two ecophysiologically dissimilar earthworm species: pollution-monitoring implications. Environ. Pollut. 82, 1–7. https://doi.org/10.1016/0269-7491(93)90155-H

Nordberg, G.F., 1989. Modulation of metal toxicity by metallothionein. Biol. Trace Elem. Res. 21, 131. https://doi.org/10.1007/BF02917245

Novo, M., Lahive, E., Díez-Ortiz, M., Matzke, M., Morgan, A.J., Spurgeon, D.J., Svendsen, C., Kille, P., 2015. Different routes, same pathways: Molecular mechanisms under silver ion and nanoparticle exposures in the soil sentinel Eisenia fetida. Environ. Pollut. 205, 385–393. https://doi.org/10.1016/j.envpol.2015.07.010

531 OCDE, 1984. Ver de terre, essai de toxicité aigüe, Ligne directrice N°207, Ligne directrice de l'OCDE pour les
532   essais de produits chimiques, OCDE, Paris.
533 Pradas del Real, A.E., Vidal, V., Carrière, M., Castillo-Michel, H., Levard, C., Chaurand, P., Sarret, G., 2017.
534   Silver Nanoparticles and Wheat Roots: A Complex Interplay. Environ. Sci. Technol. 51, 5774–5782.
535   https://doi.org/10.1021/acs.est.7b00422
536 Proux, O., Biquard, X., Lahera, E., Menthonnex, J.-J., Prat, A., Ulrich, O., Soldo, Y., Trévisson, P., Kapoujyan,
537   G., Perroux, G., Taunier, P., Grand, D., Jeantet, P., Deléglise, M., Roux, J.-P., Hazemann, J.-L., 2005.
538   FAME : A new beamline for X-ray absorption investigations of very-diluted systems of environmental,
539   material   and   biological   interests.   Phys.   Scr.   115,   970–973.
540   https://doi.org/10.1238/Physica.Topical.115a00970
541 R Core Team, 2008. R: A language and environment for statistical computing. R Foundation for Statistical
542   Computing, Vienna, Austria. URL https://www.R-project.org/
543 Ravel, B., Newville, M., 2005. ATHENA, ARTEMIS, HEPHAESTUS: data analysis for X-ray absorption
544   spectroscopy   using   IFEFFIT.   J.   Synchrotron   Radiat.   12,   537–541.
545   https://doi.org/10.1107/S0909049505012719
546 Roubalová, R., Płytycz, B., Procházková, P., Navarro Pacheco, N.I., Bilej, M., 2018. Annelida: Environmental
547   Interactions and Ecotoxicity in Relation to the Earthworm Immune System, in: Cooper, E.L. (Ed.),
548   Advances in Comparative Immunology. Springer International Publishing, Cham, pp. 933–951.
549   https://doi.org/10.1007/978-3-319-76768-0_27
550 Shoults-Wilson, W.A., Reinsch, B.C., Tsyusko, O.V., Bertsch, P.M., Lowry, G.V., Unrine, J.M., 2010. Effect of
551   silver nanoparticle surface coating on bioaccumulation and reproductive toxicity in earthworms (
552   *Eisenia fetida*). Nanotoxicology 5, 432–444. https://doi.org/10.3109/17435390.2010.537382
553 Sugawara, N., Sugawara, C., 1984. Comparative study of effect of acute administration of cadmium and silver
554   on ceruloplasmin and metallothionein: Involvement of disposition of copper, iron, and zinc. Environ.
555   Res. 35, 507–515. https://doi.org/10.1016/0013-9351(84)90157-9
556 Unrine, J., Bertsch, P., Hunyadi, S., 2008. Bioavailability, Trophic Transfer, and Toxicity of Manufactured
557   Metal and Metal Oxide Nanoparticles in Terrestrial Environments, in: Nanoscience and
558   Nanotechnology. John Wiley & Sons, Ltd, pp. 345–366. https://doi.org/10.1002/9780470396612.ch14
559 Usman, K., Khan, S., Ghulam, S., Khan, M.U., Khan, N., Khan, M.A., Khalil, S.K., 2012. Sewage Sludge: An
560   Important Biological Resource for Sustainable Agriculture and Its Environmental Implications. Am. J.
561   Plant Sci. 03, 1708–1721. https://doi.org/10.4236/ajps.2012.312209
562 Vance, M.E., Kuiken, T., Vejerano, E.P., McGinnis, S.P., Hochella, M.F., Rejeski, D., Hull, M.S., 2015.
563   Nanotechnology in the real world: Redeveloping the nanomaterial consumer products inventory.
564   Beilstein J. Nanotechnol. 6, 1769–1780. https://doi.org/10.3762/bjnano.6.181
565 Vijver, M.G., Van Gestel, C.A.M., Lanno, R.P., Van Straalen, N.M., Peijnenburg, W.J.G.M., 2004. Internal
566   metal sequestration and its ecotoxicological relevance: a review. Environ. Sci. Technol. 38, 4705–4712.
567   https://doi.org/10.1021/es040354g
568 Vijver, M.G., Vink, J.P.M., Miermans, C.J.H., van Gestel, C.A.M., 2003. Oral sealing using glue: a new method
569   to distinguish between intestinal and dermal uptake of metals in earthworms. Soil Biol. Biochem. 35,
570   125–132. https://doi.org/10.1016/S0038-0717(02)00245-6
571 Yan, A., Chen, Z., 2019. Impacts of Silver Nanoparticles on Plants: A Focus on the Phytotoxicity and
572   Underlying Mechanism. Int. J. Mol. Sci. 20, 1003. https://doi.org/10.3390/ijms20051003
573 Yu, S., Yin, Y., Liu, J., 2013. Silver nanoparticles in the environment. Env. Sci Process. Impacts 15, 78–92.
574   https://doi.org/10.1039/C2EM30595J
575

576